Chemistry–A European Journal
Research Article
doi.org/10.1002/chem.202402690
Chemistry Europe
European Chemical Societies Publishing
www.chemeurj.org

$MoSe_2$-Sensitized Water Splitting Assisted by C_{60}-Dendrons on the Basal Surface

Tomoyuki Tajima,*[a] Tomoki Matsuura,[a] Arif Efendi,[b] Mariko Yukimoto,[b] and Yutaka Takaguchi*[b]

To facilitate water splitting using $MoSe_2$ as a light absorber, we fabricated water-dispersible $MoSe_2/C_{60}$-dendron nanohybrids via physical modification of the basal plane of $MoSe_2$. Upon photoirradiation, the mixed-dimension $MoSe_2/C_{60}$ (2D/0D) heterojunction generates a charge-separated state ($MoSe_2^{\bullet+}/C_{60}^{\bullet-}$) through electron extraction from the exciton in $MoSe_2$ to C_{60}. This process is followed by the hydrogen evolution reaction (HER) from water in the presence of a sacrificial donor (1-benzyl-1,4-dihydronicotinamide) and co-catalyst (Pt-PVP). The apparent quantum yields of the HER were estimated to be 0.06% and 0.27% upon photoexcitation at the A- and B-exciton absorption peaks (λ_{max} = 800 and 700 nm), respectively.

Photocatalytic solar hydrogen production is of increasing interest as a method for converting solar energy into a chemical fuel without carbon dioxide emissions.[1] To enable scalable H_2 production, many researchers have explored the use of 2D nanomaterials as H_2 evolution photocatalysts (HEPs), since their visible- and near-IR-responsiveness and large surface area are highly promising for improving the solar energy conversion efficiency.[2,3] In this context, transition metal dichalcogenides (TMDs) are very attractive because of their unique nanosheet structure and the tunability of their band energy levels through their components.[4] However, hydrogen evolution from water photosensitized by TMDs as light-absorber is quite rare, despite the many reports of TMDs acting as efficient co-catalysts[5–8] or electron transport materials, photocatalysts consisting of light-absorbing materials and co-catalysts in TMDs,[9,10] for hydrogen generation. To use TMDs as light-absorber of particulate photocatalysts, the high binding energy (> 500 meV) of the photogenerated exciton in TMDs must be overcome to generate mobile carriers.[11] Recently, we have developed carbon nanotube (CNT) photocatalysts for HEPs by solving a similar problem.[12,13] Physical modification of semiconducting CNTs with an amphiphilic C_{60}-dendron leads to the formation of CNT/C_{60} (1D/0D) mixed-dimensional heterojunctions, which play a crucial role in electron and hole generation from excitons with high binding energies (200–500 meV).[14]

In this context, 2D/0D mixed-dimensional heterojunctions consisting of TMDs and semiconducting molecules have the potential to exhibit significant HEP activity through the formation of a charge-separated state via electron or hole extraction from excitons in the TMDs.[15–17] Recently, we have achieved efficient photoinduced charge separation between MoS_2 and anthracene using 2D/0D mixed-dimensional heterojunctions fabricated by exfoliation and surface-modification with an amphiphilic anthryl dendron.[18] The groups of Zhu and Ouyang independently reported that C_{60} can act as an efficient electron acceptor at WSe_2/C_{60} or MoS_2/C_{60} heterojunctions, demonstrating long-lived charge separation and/or photovoltaic properties.[17] This background prompted us to explore the fabrication of 2D/0D mixed-dimensional van der Waals heterojunctions based on TMDs and C_{60}-dendrons, along with their HEP activity. Herein, we propose a new class of HEPs containing TMD not as a co-catalyst, but as a photosensitizer: $MoSe_2/C_{60}$-dendron **1** nanohybrids, assisted by 1-benzyl-1,4-dihydronicotinamide (BNAH) as a sacrificial donor and Pt nanoparticles as co-catalysts.

C_{60}-dendron **1**, a dendritic dispersant that contains fullerene (C_{60}) at its focal point, was synthesized according to our previous report[17] and used for the construction of mixed-dimensional heterojunctions via the modification of fullerene molecules (0D) onto the basal surface of $MoSe_2$ (2D). Typically, a mixture of $MoSe_2$ powder (50 mg) and **1** (20 mg) in water (10 mL) was sonicated for 25 h. The suspension was then centrifuged at 3000 G for 30 min to obtain a water dispersion of $MoSe_2$/**1** nanohybrids as the supernatant (Figure 1).

Notably, Figure 1 shows a hybrid of single-layer $MoSe_2$ and C_{60}-dendron **1**, but in reality, it is a mixture containing $MoSe_2$ with various layer numbers. The synthesized $MoSe_2$/**1** nanohybrids is stable in water and does not precipitate even after 7 days, whereas $MoSe_2$ dispersion without C_{60}-dendron **1** immediately precipitates, indicating that C60-dendron **1** acts as a dispersant. There have been several reports of attractive interactions between TMDs and aromatic compounds to create

[a] Prof. T. Tajima, T. Matsuura
Graduate School of Environmental, Life, Natural Science and Technology, Okayama University, 3-1-1 Tsushima-Naka, Kita-ku, Okayama 700-8530, Japan
E-mail: tajimat@cc.okayama-u.ac.jp
[b] A. Efendi, Dr. M. Yukimoto, Prof. Y. Takaguchi
Department of Materials Design and Engineering, University of Toyama, 3190 Gofuku, Toyama, 930–8555, Japan
E-mail: tak@sus.u-toyama.ac.jp

Supporting information for this article is available on the WWW under https://doi.org/10.1002/chem.202402690

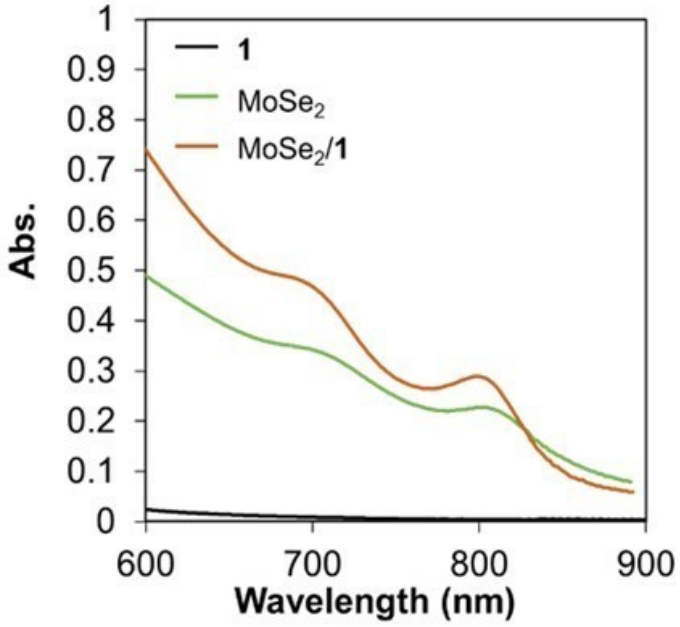

Figure 1. Schematic illustration of $MoSe_2$/**1** nanohybrids.

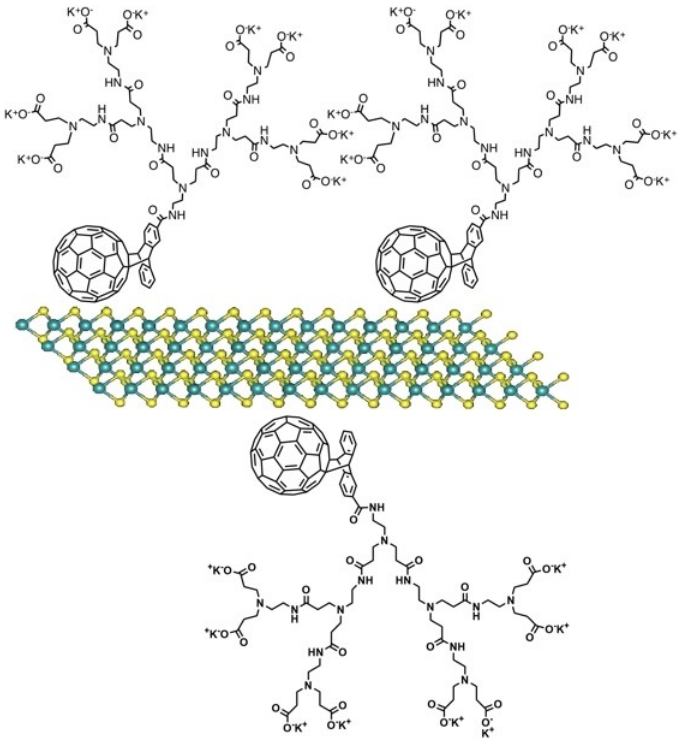

Figure 2. Visible and NIR absorption spectra of **1**, $MoSe_2$, and $MoSe_2$/**1** nanohybrids in H_2O.

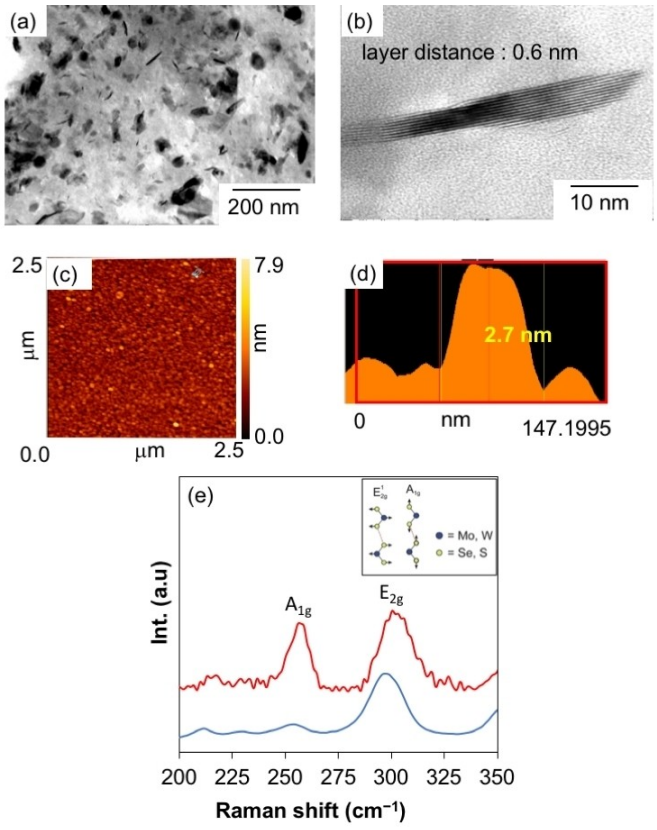

Figure 3. (a, b) TEM and (c) AFM images of $MoSe_2$/**1** nanohybrids. (d) Height profile of $MoSe_2$/**1** nanohybrids. (e) Raman spectra of $MoSe_2$/**1** nanohybrids (red) and pristine $MoSe_2$ (blue).

2D/0D heterojunctions.[18,20] It seems likely that the formation of $MoSe_2$/**1** nanohybrids leads to stable dispersion of $MoSe_2$ in water. However, no direct evidence of the formation of $MoSe_2$/**1** nanohybrids has been obtained at present. The visible and NIR absorption spectra of water dispersions of pristine $MoSe_2$ nanosheets (NSs), **1**, and $MoSe_2$/**1** nanohybrids are shown in Figure 2. The pristine $MoSe_2$ exhibited two absorbance peaks at 699 and 804 nm, corresponding to the B- and A-excitonic transitions between the split valence bands (VBs) and the minima of the conduction band (CB) at the K-point of the Brillouin zone for the $MoSe_2$ NSs (green line).[21] **1** exhibited an absorption band at 255 nm, which was ascribed to π–π^* transition, as shown in Figure S1a. The absorption spectrum of $MoSe_2$/**1** nanohybrids is in good agreement with the superposition of the spectra of $MoSe_2$ and **1** (red line). This indicates that there is no strong electronic interaction between C_{60} and $MoSe_2$ in the ground state.

$MoSe_2$/**1** nanohybrids in water remains stable and does not precipitate even after dialysis to remove the excess **1** that did not participate in the physical modification of $MoSe_2$ (Figure S1b). The typical TEM images of $MoSe_2$/**1** nanohybrids shown in Figures 3a and b indicate that the flake size ranges from 0.05–1 μm. The lattice fringe of the flake was 0.60 nm, which is identical to the theoretical layer distance of $MoSe_2$.[22] To confirm the existence of exfoliated $MoSe_2$ NSs, AFM imaging was carried out, as shown in Figures 3c and d. The height profile of the selected area shows that the thickness of $MoSe_2$/**1** nanohybrids is 2.7 nm, which is consistent with few-layer $MoSe_2$ NSs.[23] Hence, we concluded that some of the $MoSe_2$ might be exfoliated after hybridization with **1**. The $MoSe_2$ layers were further investigated by Raman spectroscopy using a 488 nm excitation laser (Figure 3e). Two typical Raman active modes, i.e., the A_{1g} Raman mode and the E_{2g} Raman mode, are

observed in the Raman spectra. The A_{1g} mode relates to the out-of-plane vibration of Se atoms, and the E_{2g} mode is associated with the in-plane vibration of Mo and Se atoms (see the inset in Figure 3e). The frequency difference between the E_{2g} and A_{1g} modes is an important indicator of the thickness of 2D materials; this difference increases as the number of layers decreases.[24] The frequency differences between E_{2g} and A_{1g} are 46.1 cm^{-1} (monolayer), 43.7 cm^{-1} (bulk), and 44.0 cm^{-1} ($MoSe_2$/**1** nanohybrids). This result also supports the exfoliation of $MoSe_2$ into few-layer NSs after hybridization with C_{60}-dendron **1**.

Figure 4 is an energy level diagram of the conduction and valence bands (CB and VB) of mono- and multi-layer $MoSe_2$,[9] the LUMO and HOMO of C_{60},[22] and the redox potentials of BNAH, MV^{2+},[25] and Pt nanoparticles (PVP–Pt). Upon photoexcitation of $MoSe_2$, electron extraction occurs from the CB of $MoSe_2$ to the LUMO of C_{60}, generating a charge-separated (CS) state ($MoSe_2^{\bullet+}$/$\mathbf{1}^{\bullet-}$). Subsequently, the hole in the CS state oxidizes BNAH, while the electron participates in the H_2 evolution reaction via electron transfer to Pt nanoparticles facilitated by the electron relay MV^{2+}. We attempted to confirm the photoinduced electron extraction from $MoSe_2$ to C_{60} of **1** through fluorescence quenching of $MoSe_2$. However, we did not detect any emission from $MoSe_2$, presumably due to incomplete exfoliation. The electron transfer from $C_{60}^{\bullet-}$ in the CS state to MV^{2+} was confirmed through the observation of $MV^{\bullet+}$, the one-electron reduction product of MV^{2+}, using absorption spectroscopy under illumination ($\lambda_{ex} > 422$ nm) (Figure S2). It should be noted that that only monolayer or few-layer $MoSe_2$ possesses photosensitization ability. However, the $MoSe_2$/**1** nanohybrids used in our study contain $MoSe_2$ layers of varying thicknesses (ranging from single-layer to multi-layer). The energy levels of the VB and CB of $MoSe_2$ are known to vary with the number of layers. Single or few-layer $MoSe_2$ favors photoinduced electron transfer from the CB of $MoSe_2$ (−0.61 V)[11] to the LUMO of C_{60} (−0.5 V),[22] because the CB energy level of a single layer of $MoSe_2$ is higher than that of the LUMO of C_{60}. In contrast, multi-layer $MoSe_2$ is less likely to generate a CS state, because the energy level of the CB of multi-layer $MoSe_2$ (−0.38 V, shown as a dotted line in Figure 4) is lower than that of the LUMO of C_{60}. The fabrication of $MoSe_2$/**1** nanohybrids consisting of solely monolayer or few-layer $MoSe_2$ is crucial for enhancing photocatalytic H_2 production. However, we have not yet succeeded in fabricating such $MoSe_2$/**1** nanohybrids. Detailed reports on this endeavor will be provided in the future.

In order to evaluate the HER activity of the $MoSe_2/C_{60}$ nanohybrid photocatalysts for the construction of a water splitting system, we investigated the HER using $MoSe_2$/**1** nanohybrids in the presence of BNAH, MV^{2+} and Pt-PVP as a sacrificial donor, electron mediator, and co-catalyst, respectively, upon selective photo-excitation with monochromatic light at 800 nm, which corresponds to the A-exciton absorption of $MoSe_2$ (Figure 5). Although H_2 production did not proceed under the dark conditions during the first hour, steady generation of H_2 (1.1 μmol/h) without an induction period or a decrease in activity was observed during the subsequent 7 h of irradiation (Figure 5a), and the apparent quantum yield (AQY) of the HER was estimated to be 0.06 %. Under light irradiation at 700 nm, which corresponds to the absorption band of the B-exciton in $MoSe_2$, the hydrogen generation rate was 1.5 μmol/h with an AQY of 0.26 %. The hydrogen evolution rates in the presence and absence of the $MoSe_2$/**1** nanohybrids were compared under visible light irradiation ($\lambda_{ex} > 422$ nm). H_2 evolution (70 μmol/h, 280,000 μmol h^{-1} g^{-1}) was observed in the presence of $MoSe_2$/**1** (Figure 5b, i) but not in the absence of $MoSe_2$/**1** nanohybrids (Figure 5b, iii). Therefore, the 2D/0D heterojunction ($MoSe_2/C_{60}$) plays a crucial role in this water splitting reaction. Moreover, the H_2 evolution rate of $MoSe_2$/**1** nanohybrids (280,000 μmol h^{-1} g^{-1}) is higher than that of light-absorber/$MoSe_2$-co-catalyst system such as eosin Y/$MoSe_2$ (62,000 μmol h^{-1} g^{-1})[9] and poly(diallyldimethylammonium chloride)-functionalized reduced graphene oxide/$MoSe_2$ (9,705 μmol h^{-1} g^{-1}).[10] It demonstrates that $MoSe_2$ light-absorber can function at high efficiencies without the need for dye-sensitization. Additionally, when $MoSe_2$ was used instead of $MoSe_2$/**1** nanohybrids, the H_2 evolution activity was quite low (1.2 μmol/h, Figure 5b, ii) due to the low efficiency of direct electron extraction from the exciton in $MoSe_2$ to MV^{2+}. We then examined the variation in the quantity of hydrogen generated as a function of the pH value under visible light irradiation at

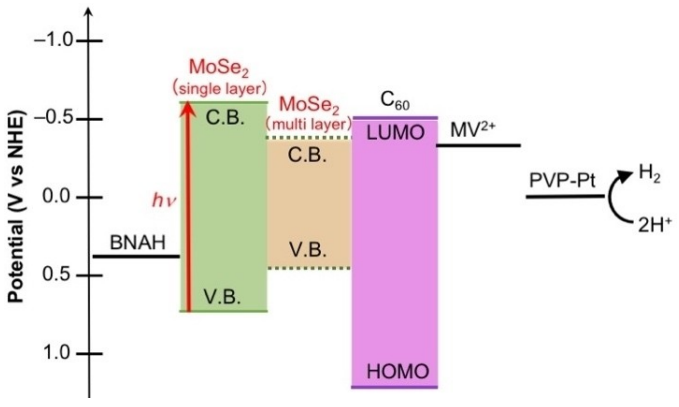

Figure 4. Energy level diagram for water splitting using $MoSe_2$/**1** nanohybrids.

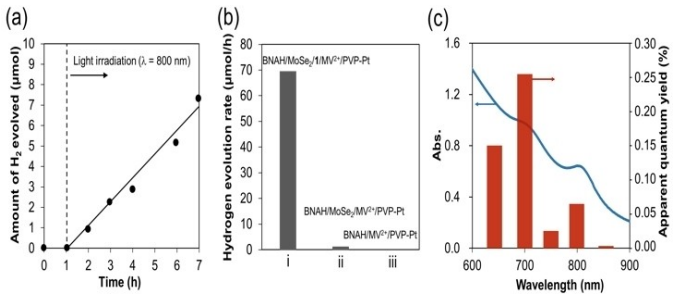

Figure 5. (a) Time course of H_2 evolution from water using $MoSe_2$/**1** nanohybrids ($\lambda = 800$ nm). (b) H_2 evolution rate in the presence and absence of $MoSe_2$/**1** nanohybrids ($\lambda > 422$ nm). The tested systems are: (i) BNAH/$MoSe_2$/**1**/MV^{2+}/PVP–Pt, (ii) BNAH/$MoSe_2$/MV^{2+}/PVP–Pt, and (iii) BNAH/MV^{2+}/PVP–Pt. (c) Absorption spectrum of $MoSe_2$/**1** nanohybrids in H_2O and action spectrum of H_2 evolution from water using $MoSe_2$/**1** nanohybrids as the photocatalyst.

pH 1, 2.5, 5, 7.5, and 9. The highest activity was observed at pH 2.5, with the activity decreasing as the solution approached basic conditions (Figure S3). This phenomenon was attributed to the negative shift in the hydrogen generation potential as the solution becomes more alkaline. In addition, an action spectrum was obtained to confirm the photosensitizer in this photocatalytic system. Figure 5c shows the action spectrum for the evolution of H_2 using the $MoSe_2$/**1** nanohybrids under various monochromatic wavelengths (650, 700, 760, 800 and 860 nm), along with the UV-vis spectrum of $MoSe_2$. The obtained action spectrum closely matches the absorbance profile of $MoSe_2$. The two AQY peaks (0.26% at 700 nm, 0.06% at 800 nm) were coincident with the two absorption bands of $MoSe_2$, i.e., the A- and B-excitonic transitions (804 and 699 nm). This result indicates that $MoSe_2$ is the light absorber in this photosensitizing system.

In conclusion, water-dispersible $MoSe_2/C_{60}$-dendron nanohybrids were successfully prepared *via* the physical modification of $MoSe_2$ with C_{60}-dendron **1**. The 2D/0D mixed-dimensional heterojunction formed by $MoSe_2$ and C_{60} is highly effective in generating mobile carriers under visible and NIR light irradiation. This process involves electron extraction from the exciton in $MoSe_2$ to C_{60}, followed by electron transfer to Pt nanoparticles via MV^{2+}, leading to H_2 production from water. Notably, even NIR light, such as 800 nm light corresponding to the A-exciton absorption of $MoSe_2$, can facilitate water splitting. The EQY of the H_2 evolution reaction was estimated to be 0.0027% in the presence of BNAH as a sacrificial donor. The successful H_2 evolution from water through the fabrication of a 2D/0D mixed-dimensional heterojunction highlights the potential of TMDs as light absorbers. Further studies on TMD-photocatalysts with mixed-dimensional heterojunctions are underway in our group to develop Z-scheme photocatalytic systems for solar fuel production and improve solar-to-hydrogen conversion efficiency.

Supporting Information Summary

The data that support the finding of this study are available in the supplementary material of this paper.

Acknowledgements

This work was partially supported by Ame Hisaharu Foundation and JSPS KAKENHI grants 23K04778 (T. T.) and 23K04519, 24H01616 (Y. T.).

Conflict of Interests

The authors declare no conflict of interest.

Data Availability Statement

The data that support the findings of this study are available on request from the corresponding author. The data are not publicly available due to privacy or ethical restrictions.

Keywords: Water splitting · Transition metal dichalcogenide · Hydrogen evolution · Photocatalyst · Fullerene

[1] a) T. Hisatomi, K. Domen, *Nat. Catal.* **2019**, *2*, 387; b) H. Nishiyama, T. Yamada, M. Nakabayashi, Y. Maehara, M. Yamaguchi, Y. Kuromiya, Y. Nagatsuma, H. Tokudome, S. Akiyama, T. Watanabe, R. Narushima, S. Okunaka, N. Shibata, T. Takata, T. Hisatomi, K. Domen, *Nature* **2021**, *598*, 304.
[2] a) D. Deng, K. S. Novoselov, Q. Fu, N. Zheng, Z. Tian, X. Bao, *Nat. Nanotechnol.* **2016**, *11*, 218; b) C. Tan, X. Cao, X. -J. Wu, Q. He, J. Yang, X. Zhang, J. Chen, W. Zhao, S. Han, G. -H. Nam, M. Sindoro, H. Zhang, *Chem. Rev.* **2017**, *117*, 6225; c) K. Maeda, T. E. Mallouk, *Bull. Chem. Soc. Jpn.* **2019**, *92*, 38; d) H. Hou, X. Zeng, X. Zhang, *Sci. China Mater.* **2020**, *63*, 2119; e) H. Yu, M. Dai, J. Zhang, W. Chen, Q. Jin, S. Wang, Z. He, *Small* **2023**, *19*, 2205767; f) Y. N. Teja, M. Sakar, *Small* **2023**, *19*, 2303980; g) G. Zhang, S. Huang, X. Li, D. Chen, N. Li, Q. Xu, H. Li, J. Lu, *Appl. Catal. B* **2023**, *331*, 122725; h) B. Zhu, J. Sun, Y. Zhao, L. Zhang, J. Yu, *Adv. Mater.* **2024**, *36*, 2310600.
[3] a) M. Zhu, Z. Sun, M. Fujitsuka, T. Majima, *Angew. Chem. Int. Ed.* **2018**, *57*, 2160; b) X. Shi, L. Mao, P. Yang, H. Zheng, M. Fujitsuka, J. Zhang, T. Majima, *Appl. Catal. B* **2020**, *265*, 118616; c) D. Ruan, M. Fujitsuka, T. Majima, *Appl. Catal. B* **2020**, *264*, 118541; d) J. Du, Y. Shen, F. Yang, J. Wei, K. Xu, X. Li, C. An, *Appl. Surf. Sci.* **2023**, *608*, 155199.
[4] J. Kang, S. Tongay, J. Zhou, J. Li, J. Wu, *Appl. Phys. Lett.* **2013**, *102*, 012111.
[5] a) W. Peng, Y. Li, F. Zhang, G. Zhang, X. Fan, *Ind. Eng. Chem. Res.* **2017**, *56*, 4611; b) C. K. Sumesh, S. C. Peter, *Dalton Trans.* **2019**, *48*, 12772; c) Y. Jiang, H. Sun, J. Guo, Y. Liang, P. Qin, Y. Yang, L. Luo, L. Leng, X. Gong, Zhibin Wu, *Small* **2024**, *20*, 2310396.
[6] R. Yang, Y. Fan, Y. Zhang, L. Mei, R. Zhu, J. Qin, J. Hu, Z. Chen, Y. Hau Ng, D. Voiry, S. Li, Q. Lu, Q. Wang, J. C. Yu, Z. Zeng, *Angew. Chem. Int. Ed.* **2023**, *62*, e202218016.
[7] a) Y. Wang, S. Zhao, Y. Wang, D. A. Laleyan, Y. Wu, B. Ouyang, P. Ou, J. Song, Z. Mi, *Nano Energy* **2018**, *51*, 54; b) Y. Pang, M. N. Uddin, W. Chen, S. Javaid, E. Barker, Y. Li, A. Suvorova, M. Saunders, Z. Yin, G. Jia, *Adv. Mater.* **2019**, *31*, 1905540.
[8] a) Y. Fan, J. Wang, M. Zhao, *Nanoscale* **2019**, *11*, 14836; b) R. Canton-Vitoria, T. Hotta, Y. Tanuma, I. K. Sideri, N. Tagmatarchis, C. Ewels, R. Kitaura, *J. Phys. Chem. C* **2023**, *127*, 10699; c) G. Shao, J. Xu, S. Gao, Z. Zhang, S. Liu, X. Zhang, Z. Zhou, *Carbon Energy* **2024**, *6*, e417; d) Y. Qian, J. Yu, Z. Lyu, Q. Zhang, T. H. Lee, H. Pang, D. J. Kang, *Carbon Energy* **2024**, *6*, e376.
[9] U. Gupta, B. S. Naidu, U. Maitra, A. Singh, S. N. Shirodkar, U. V. Waghmare, C. N. R. Rao, *APL Mater.* **2014**, *2*, 092802.
[10] K. Pramoda, S. Servottam, M. Kaur, C. N. R. Rao, *ACS Appl. Nano Mater.* **2020**, *3*, 1792.
[11] T. Mueller, E. Malic, *NPJ 2D Mater. Appl.* **2018**, *2*, 29.
[12] a) T. Tajima, W. Sakata, T. Wada, A. Tsutsui, S. Nishimoto, M. Miyake, Y. Takaguchi, *Adv. Mater.* **2011**, *23*, 5750; b) Y. Sasada, T. Tajima, T. Wada, T. Uchida, M. Nishi, T. Ohkubo, Y. Takaguchi, *New J. Chem.* **2013**, *37*, 4214; c) K. Kuruniawan, T. Tajima, Y. Kubo, H. Miyake, W. Kurashige, Y. Negishi, Y. Takaguchi, *RSC Adv.* **2017**, *7*, 31767; d) N. Murakami, Y. Tango, H. Miyake, T. Tajima, Y. Nishina, W. Kurashige, Y. Negishi, Y. Takaguchi, *Sci. Rep.* **2017**, *7*, 43445; e) K. Ishimoto, T. Tajima, H. Miyake, M. Yamagami, W. Kurashige, Y. Negishi, Y. Takaguchi, *Chem. Commun.* **2018**, *54*, 393; f) T. Izawa, V. Kalousek, D. Miyamoto, N. Murakami, H. Miyake, T. Tajima, W. Kurashige, Y. Negishi, K. Ikeue, T. Ohkubo, Y. Takagichi, *Chem. Lett.* **2019**, *48*, 410; g) M. Yamagami, T. Tajima, Z. Zhang, J. Kano, K.-I. Yashima, T. Matsubayashi, H. K. Nguyen, N. Nishiyama, T. Hayashi, Y. Takaguchi, *Nanomaterials* **2022**, *12*, 3826.
[13] a) N. Murakami, H. Miyake, T. Tajima, K. Nishikawa, R. Hirayama, Y. Takaguchi, *J. Am. Chem. Soc.* **2018**, *140*, 3821; b) T. Tajima, M. Yamagami, R. Sagawa, H. Miyake, Y. Takaguchi, *J. Appl. Phys.* **2021**, *129*, 014303; c) H. Watanabe, K. Ekuni, Y. Okuda, R. Nakayama, K. Kawano, T. Iwanaga, A. Yamaguchi, T. Kiyomura, H. Miyake, M. Yamagami, T. Tajima,

T. Kitai, T. Hayashi, N. Nishiyama, Y. Kusano, H. Kurata, Y. Takaguchi, A. Orita, *Bull. Chem. Soc. Jpn.* **2023**, *96*, 57.
[14] F. Wang, G. Dukovic, L. E. Brus, T. F. Heinz, *Science* **2005**, *308*, 838.
[15] D. M. de Clercq, J. Yang, M. Hanif, J. Alves, J. Feng, M. P. Nielsen, K. Kalantar-Zadeh, T. W. Schmidt, *J. Phys. Chem. C* **2023**, *127*, 11260.
[16] T. Scharl, G. Binder, X. Chen, T. Yokosawa, A. Cadranel, K. C. Knirsch, E. Spiecker, A. Hirsch, D. M. Guldi, *J. Am. Chem. Soc.* **2022**, *144*, 5834.
[17] a) C. Zhao, W. Tao, Z. Chen, H. Zhou, C. Zhang, J. Lin, H. Zhu, *J. Phys. Chem. Lett.* **2021**, *12*, 3691; b) B. Cai, Y. Zhao, Z. Zhang, G. Ouyang, *Phys. Status Solidi RRL* **2021**, *15*, 2100311.
[18] T. Tajima, S. Okabe, Y. Takaguchi, *Bull. Chem. Soc. Jpn.* **2020**, *93*, 745.
[19] Y. Takaguchi, Y. Sako, Y. Yanagimoto, S. Tsuboi, J. Motoyoshiya, H. Aoyama, T. Wakahara, T. Akasaka, *Tetrahedron Lett.* **2003**, *44*, 5777.
[20] a) G. Guan, S. Zhang, S. Liu, Y. Cai, M. Low, C. P. Teng, I. Y. Phang, Y. Cheng, K. L. Duei, B. M. Srinivasan, Y. Zheng, Y. Zheng, M. Han, *J. Am. Chem. Soc.* **2015**, *137*, 6152; b) C. Zhang, D. Hu, J. Xu, M. Xu, M. Ma, K. Yao, J. Ji, Z. Xu, *ACS Nano* **2018**, *12*, 12347.
[21] M. S. Hassan, P. Basera, S. Bera, M. Mittal, S. K. Ray, S. Bhattacharya, S. Sapra, *ACS Appl. Mater. Interfaces* **2020**, *12*, 7317.
[22] Z. Sun, H. Chu, Y. Li, L. Liu, S. Zhao, G. Li, D. Li, *Opt. Mater. Express* **2019**, *9*, 3494.
[23] Y. Sha, S. Xiao, X. Zhang, F. Qin, X. Gu, *Appl. Surf. Sci.* **2017**, *411*, 182.
[24] J. Xia, X. Huang, L.-Z. Liu, M. Wang, L. Wang, B. Huang, D.-D. Zhu, J.-J. Li, C.-Z. Gu, X.-M. Meng, *Nanoscale* **2014**, *6*, 8949.
[25] S. Fukuzumi, S. Koumitsu, K. Hironaka, T. Tanaka, *J. Am. Chem. Soc.* **1987**, *109*, 305.

Manuscript received: July 15, 2024
Accepted manuscript online: September 11, 2024
Version of record online: ■■, ■■

RESEARCH ARTICLE

Upon photoirradiation of a water dispersion of $MoSe_2/C_{60}$-dendron nanohybrids, the hydrogen evolution reaction (HER) proceeded in the presence of a sacrificial donor (1-benzyl-1,4-dihydronicotinamide) and co-catalyst (Pt-PVP). The apparent quantum yields of the HER were estimated to be 0.06% and 0.27% upon photoexcitation at the A- and B-exciton absorption peaks (λ_{max} = 800 and 700 nm), respectively.

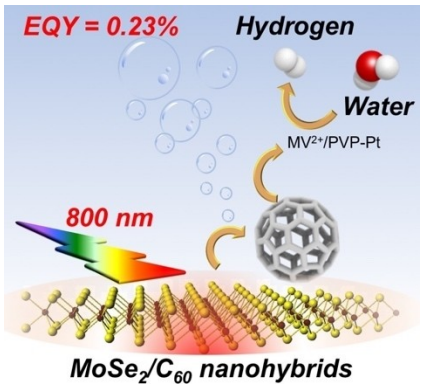

Prof. T. Tajima, T. Matsuura, A. Efendi, Dr. M. Yukimoto, Prof. Y. Takaguchi**